LAWRENCE
LIVERMORE
NATIONAL
LABORATORY

LLNL-JRNL-648161

Equilibrium Thermodynamics of helium in delta-phase Pu-Ga alloys

A. V. Karavaev, V. V. Dremov, G. V. Ionov, B. W. Chung

January 2, 2014

Acta Materialia

Disclaimer

This document was prepared as an account of work sponsored by an agency of the United States government. Neither the United States government nor Lawrence Livermore National Security, LLC, nor any of their employees makes any warranty, expressed or implied, or assumes any legal liability or responsibility for the accuracy, completeness, or usefulness of any information, apparatus, product, or process disclosed, or represents that its use would not infringe privately owned rights. Reference herein to any specific commercial product, process, or service by trade name, trademark, manufacturer, or otherwise does not necessarily constitute or imply its endorsement, recommendation, or favoring by the United States government or Lawrence Livermore National Security, LLC. The views and opinions of authors expressed herein do not necessarily state or reflect those of the United States government or Lawrence Livermore National Security, LLC, and shall not be used for advertising or product endorsement purposes.

Equilibrium thermodynamics of helium in δ-phase Pu-Ga alloys

A. V. Karavaev[1], V. V. Dremov, G. V. Ionov

Russian Federal Nuclear Center - Zababakhin Institute of Technical Physics (RFNC-VNIITF), 13, Vasiliev st., Snezhinsk, Chelyabinsk reg., Russia, 456770

B. W. Chung

Lawrence Livermore National Laboratory, Livermore, CA 94551, USA

Abstract

The paper is devoted to a theoretical study by the means of classical molecular dynamics into the response of δ-phase Pu-Ga alloys on self-irradiation. We have investigated the behavior of He atoms in the fcc lattice of Pu-Ga alloy at the ambient conditions. Because of the relatively low diffusive mobility of He atoms in the Pu-Ga alloy lattice their dynamics cannot be tracked in direct classical molecular dynamics simulations. Instead, we use the Helmholtz free energy function to investigate the equilibrium thermodynamics of metastable states (micro-configurations) in an initially perfect Pu-Ga crystal and perfect crystals with artificially introduced He atoms in different configurations. The Helmholtz free energy of metastable micro-configurations is calculated using thermodynamic integration method which is shown to be effective, accurate and thermodynamically consistent through a set of numerical tests. Thermodynamic integration technique is used to calculate the free energy of the fcc δ-phase Pu-Ga alloy with distributed He atoms as disordered substitutional atoms and with He bubbles of different sizes with various He concentrations (number of He atoms per vacant site). Based on the resulted absolute values of free energy the inferences about the relative thermodynamic stability of dif-

[1] a.v.karavayev@vniitf.ru

ferent micro-configurations at the ambient conditions are drawn. Estimates of the equilibrium parameters of He bubbles in the fcc lattice of Pu-Ga alloys and distribution of He bubble radii are calculated and compared to those observed experimentally with transmission electron microscopy.
Keywords: δ-phase Pu-Ga alloys, self-irradiation, radioactive aging, He bubbles, classical molecular dynamics, thermodynamic potentials, free energy, thermodynamic integration

1. Introduction

One of the most extensively studied during the past decades material science problems is the degradation of structural materials properties due to irradiation and radioactive materials physical properties changes due to self-irradiation known as radioactive aging. This problem is of great importance for nuclear applications. The self-irradiation of α-active actinide elements and their alloys and compounds results in continuous production of radiogenic helium and primary radiation defects (PRD) of crystal structure, their accumulation, diffusive migration in the lattice, clustering *etc.* The microstructure (morphology) of the point defect clusters (*i.e.* equilibrium size of defect clusters, their shapes, the fraction of free and clustered defects) is the subject of great importance, since it has direct impact on the properties of the materials such as elastic-plastic properties, static and dynamic strength, transport coefficients *etc.* The present study is devoted to the investigation into the behavior of one of the products of the α-decay of ^{239}Pu, namely, He atoms accumulated in the fcc lattice of δ-phase Pu-Ga alloys during long-time storage at the ambient conditions. According to [1, 2, 3, 4] the accumulation of helium with constant rate ~ 41 *ppm* per year [1] could potentially significantly affect the properties of Ga stabilized δ-Pu. According to estimates after 50 years of storage He concentration in Pu-Ga alloys is close to 2000 *ppm*. That is in 1 *kg* of plutonium there are ~ 0.2 liters of He (measured at the ambient conditions). It is well known that considerably lower amount of helium (≥ 100 *ppm*) in fcc stainless steels causes swelling and

significant embrittlement.

α-particles produced in the α-decay with the energy $\sim 5\ MeV$ lose the most of the kinetic energy trough electronic excitations, grab two electrons, and become neutral He atoms, which occupy the nearest vacancies in the fcc lattice of Pu-Ga alloys or create and occupy vacant sites by knocking out Pu or Ga lattice atoms generating interstitials [5, 6, 7, 8]. Diffusive migration of secluded He atoms in the fcc lattice of Pu-Ga alloys occurs as a motion of He atom-vacancy complex with a rather high compared to the ambient temperature diffusive activation energy $\sim 0.7\ eV$ [6]. If two diffusing He atom-vacancy complexes meet, then a nucleus of He gas bubble is formed.

The first observation of helium bubbles in naturally aged material reported in [9, 10] was made with the transmission electron microscopy (TEM) of 21-year old δ-phase Pu-Ga alloy annealed at 400^oC for 1 hour. Recently Schwartz and coworkers studied δ-phase Pu-Ga alloy samples with ages ranging from 6 month to 42 years using a Fresnel fringe imaging technique on LLNL 300 keV TEM in combination with positron annihilation spectroscopy [11, 12, 13, 14, 15]. In the old samples aged at the ambient conditions authors observed that the dominant defects are nanometer-sized helium bubbles, which are distributed homogeneously in the bulk of fcc Pu-Ga crystal, while they found no helium bubbles in 6-month old sample with the sizes higher than their spatial resolution $0.7\ nm$. For the 16 to 42-year old samples obtained number density of helium bubbles is in the range $0.6-2.0\times10^{17}cm^3$, which increases with the sample ages at nearly steady rate. Observed average size of helium bubbles is $\sim 1.4\ nm$, and this value almost does not change with material age between 16 and 42 years. The volume fraction of helium bubbles increased from ~ 0.01 to ~ 0.03 % within the age range from 16 to 42 years. With additional measurements using positron annihilation spectroscopy and theoretical analysis by Howell and Sterne (Howell and Sterne 2002, private communication to Schwartz), Schwartz *et al.* concluded that helium bubbles contain two to three helium atoms per vacant site. Moreover, the characteristic positron lifetime of $180-190\ ps$ remains remarkably constant for all aged material, implying that equilibrium helium

density within the bubbles of 2 to 3 helium atoms per vacant site remains nearly constant at the ambient conditions.

More recently Jeffries *et al.*[16] have performed TEM study of aged (20 and 42-year old) samples of Pu-3 *at*. % Ga alloy using the same method as previously [11, 14, 15] in order to evaluate the mechanism of helium bubble coarsening. After initial characterization authors annealed the samples in vacuum at temperatures from 250^oC to 425^oC during periods from 2 to 90 hours. Then the samples were cooled down to the room temperature and examined in the TEM. In addition time-resolved *in situ* TEM microphotographs of 42-year old samples were taken during the annealing at 450^oC using a Gatan hot stage. There are two mechanisms of helium bubble coarsening generally thought to occur [17]: so called Ostwald ripening (OR), when the bubbles are thought to expand due to individual He atoms diffusive motion trough the crystal from the smaller bubbles to the larger ones [18], and bubble migration and coalescence (MC) mechanism, when helium migration in the lattice occurs as motion of the whole bubbles themselves, and the bubbles grow by coalescing when they meet one another [19]. In [16] authors conclude that carried out TEM experiments suggest that in naturally aged δ-pase Pu-Ga alloys the annealing causes coarsening of helium bubbles, decreasing the overall number density of the bubbles in the material and increasing their average size. There is clear time and temperature dependence of the bubble coarsening. The time-resolved *in situ* TEM microphotographs evidence bubble migration and coalescence, providing confidence that MC is the dominating mechanism of helium bubble coarsening.

Thermally activated time-dependent growth of helium bubbles at the elevated temperatures, migration of helium bubbles as whole in the lattice of Pu-Ga alloys, strongly peaked distribution of helium bubble diameters, and nearly constant He atom to vacancy ratio in naturally $16-42$-year old aged material at the ambient conditions suggest that there are factors limiting the growth process and defining equilibrium parameters of the bubbles. In the following sections we investigate the questions of solubility of helium in the fcc lattice of δ-phase Pu-Ga alloys, nature of attractive/repulsive interaction of He atoms with He

bubbles, possible mechanism limiting the size of the bubbles, equilibrium bubble parameters (size and He concentration - number of He atoms per vacant site) at the ambient conditions by the means of Classical Molecular Dynamics (CMD).

While the dynamics of interstitial atoms in fcc lattice of Pu-Ga alloys due to their high mobility is accessible for direct CMD simulations even at temperatures below ambient [20, 21], characteristic activation energies for the motion of vacancies and He atoms are rather high [6, 20], and consequently at room temperature diffusive migration times of vacancies and He atoms are in the range from seconds to hours, which makes it impossible to model their diffusive dynamics directly even using accelerated CMD. Instead in the present study we propose to investigate relative thermodynamic stability of metastable micro-configurations of an ideal crystal with artificially introduced systems of defects of various morphology using the Helmholtz free energy.

2. Free Energy Calculations in CMD

For the investigation into relative thermodynamic stability at finite temperatures it is insufficient to calculate and compare only the internal energies of different states. At the finite temperatures the entropy term of the Helmholtz free energy plays an important role. If one could calculate "absolute" values of free energies for different metastable micro-configurations of a system for the same external conditions, it would become possible to draw unambiguous conclusions about relative thermodynamic stability of those states for the given conditions. Unfortunately the absolute values of free energy can not be calculated in simple CMD simulation as an average of some quantity or expressed as a function of some averages. However, it is possible to evaluate the absolute values of free energy in the frames of CMD approach using so called thermodynamic integration method (TIM) [22, 23, 24].

2.1. Thermodynamic Integration Method

For the purpose of the paper we think it is necessary to remaind the general ideas of the thermodynamic integration method by Frenkel and Laad [22, 23, 24] and represent some of the mathematical relations of the method, since we are going to refer to them in the following sections of the paper. Here we abide by the notations and formulations of [24]. Classical theory of phase equilibria is based on the comparison of thermodynamic potentials. The second law of thermodynamics can be formulated as following. In an isolated system with internal energy E, a volume V, and fixed number of particle N (NVE or microcanonical ensemble) in thermodynamic equilibrium entropy S has maximal value. From such formulation one can easily deduce [25, 26] similar criteria for the systems which can exchange energy, particles or volume with external reservoir. Particularly for NVT-ensemble (canonical Gibbs ensemble) Helmholtz free energy F has its minimum in a state of thermodynamic equilibrium, and for NPT-ensemble thermodynamic Gibbs potential ($G = F + PV$) is minimal. None of these thermodynamic potentials can be "measured" directly in a simple CMD simulation (neither in real experiments).

Helmholtz free energy F of a system of N equivalent particles put in a constant volume V at a temperature T is calculated using canonical distribution function

$$\begin{aligned} F &= -k_B T \ln Z_N\left(V,T\right) \\ &\equiv -k_B T \ln \left(\frac{\int\limits_{\Gamma} d\mathbf{p}^N d\mathbf{r}^N \exp\left(-\frac{H\left(\mathbf{p}^N,\mathbf{r}^N\right)}{k_B T}\right)}{h^{dN} N!} \right), \end{aligned} \tag{1}$$

where k_B - Boltzmann constant, h - Plank constant, d - dimensionality of space, H - Hamilton function of the system. The integration is to be done over the entire available phase space Γ, but not over that covered in a particular numerical simulation. The factor h^{dN} is the norm of phase space volume. Generally speaking, in classical statistical physics entropy is determined up to an additive constant, and as the norm of pase space volume one can use any constant with

the dimension of action powered dN. The use of Plank constant h as the norm of the phase space volume in classical statistical physics dictated by the reason that in that case all the equations of classical statistics can be obtained from quantum statistics equations in the limit $T \to \infty$ [25, 26]. The main problem of the statistical physics is the calculation of the integral in Eq. (1) called statistical integral $Z_N(V,T)$. In general case it can not be expressed as a function of some canonical averages, that is why free energy, entropy, and Gibbs potential can not be measured in a numerical experiment in a simple manner.

Following Frenkel and Laad[22, 23, 24] let consider a system of N particles in a volume V interacting through artificial interatomic potential U. Let construct U such that it linearly depends on coupling parameter λ changing in the range from 0 to 1, and for $\lambda = 0$ potential U becomes a potential U_I, for which we somehow can calculate the free energy value, while for $\lambda = 1$ potential U becomes U_{II} - the potential of interest for which we want to calculate thermodynamic potential values

$$U = (1-\lambda)\, U_I + \lambda U_{II}. \tag{2}$$

If one uses the model potential U to calculate statistical integral $Z_N(V,T)$, and take the integral in the momentum part of the phase space, one obtains

$$Z_N(V,T,\lambda) = \frac{1}{(\Lambda_T)^{dN}\, N!} \int\limits_{V^N} d\mathbf{r}^N \exp\left(-\frac{U(\lambda, \mathbf{r}^N)}{k_B T}\right), \tag{3}$$

where $\Lambda_T = h/\sqrt{2\pi m k_B T}$ thermal de Broglie wavelength. For the model potential U partial derivative of free energy F with respect to coupling parameter λ is

$$\left(\frac{\partial F(\lambda)}{\partial \lambda}\right)_{N,V,T} = \left\langle \frac{\partial U(\lambda)}{\partial \lambda} \right\rangle_\lambda = \langle U_{II} - U_I \rangle_\lambda, \tag{4}$$

where $\langle \ldots \rangle_\lambda$ means canonical average value at a fixed value of coupling parameter λ. Finally, free energy of the state of interest ($\lambda = 1$) can be calculated as

$$F(\lambda = 1) = F(\lambda = 0) + \int\limits_0^1 d\lambda \, \langle U_{II} - U_I \rangle_\lambda. \tag{5}$$

So, we expressed free energy of the state of interest as a sum of free energy of a reference state, for which we can calculate somehow thermodynamic potential values, and the function of canonical averages, which can be calculated in numerical experiments. In principle, there is no need to use the linear combination of U_I and U_{II} (2) as the model potential U. We could use as model potential U any function of coupling parameter λ satisfying boundary conditions $U = U_I$ for $\lambda = 0$ and $U = U_{II}$ for $\lambda = 1$ and differentiable at $0 \leq \lambda \leq 1$. However the using of the linear combination (2) is useful from the practical point and provides additional instrument to control correctness of results of numerical simulations. If one takes derivative of Eq. (4) with respect to λ, one gets

$$\frac{\partial^2 F}{\partial \lambda^2} = -\frac{\left\langle (U_{II} - U_I)^2 \right\rangle_\lambda - \langle U_{II} - U_I \rangle_\lambda^2}{k_B T} \leq 0. \tag{6}$$

That is the derivative $\partial F/\partial \lambda$ (that is value of $\langle U_{II} - U_I \rangle_\lambda$) can not increase with increasing λ. Inequality (6) (Gibbs-Bogolubov inequality) should be used in numerical simulations to control the correctness of results.

In order to obtain the value of free energy for the system of interest the transition from the reference state ($\lambda = 0$) to the state of interest ($\lambda = 1$) should be done along quasi-equilibrium reversible thermodynamic path where the parameters of the system should be changed slowly enough in quasi-adiabatic manner. In practice the integration in Eq. (5) should be done numerically for discrete values of coupling parameter λ, and of course it can be done only if the kernel of the integral is "good" for all $0 \leq \lambda \leq 1$. In general, the linear interpolation (2) could lead to a weak and relatively harmless singularity of the kernel for example when one of the potentials U_I or U_{II} is singular in the case of particle separation going to 0 (for example Lennard-Jones potential, exp 6 potential). The singularity if it appears usually does not affect the convergence of the integral in Eq. (5) and/or can be avoided by special tricks.

2.2. Free Energy of Pu-Ga Alloys with He Atom-Vacancy Complexes

So far we did not specify the form of the potential of the reference system U_I. It is clear that the form of the potential U_I should be chosen based on the

properties of the state of interest with the main requirements that for the reference state one can obtain values of thermodynamic potentials, and there should be quasi-equilibrium reversible thermodynamic path (without phase transitions) from the reference state to the state of interest. In this section we present detailed description with examples of the free energy calculations for Pu-Ga alloys with He atoms in the form of bubbles and He atom-vacancy complexes.

In a crystalline solid particles spend almost all the time near their equilibrium positions in the lattice nodes. The rms deviations of atoms from their equilibrium positions are defined by interatomic interactions and the state of the crystal (stresses and its temperature). Since we are considering a crystal in classical (non-quantum) statistics approximation, it is quite natural to use as the reference state the Einstein harmonic crystal in the high temperature limit, *i.e.*

$$U_I\left(\mathbf{r}_i\right) = \sum_{i=1}^{N} \frac{\alpha_i}{2}\left(\mathbf{r}_i - \mathbf{r}_i^{(0)}\right)^2 + U_{II}^{(0)}, \tag{7}$$

where $\mathbf{r}_i^{(0)}$ are equilibrium atomic positions at $\lambda = 1$, and α_i are effective harmonic force constants which are, in general, free parameters of the method and can take almost arbitrary values with the only requirement that atoms are effectively held near their equilibrium positions $\mathbf{r}_i^{(0)}$ during the entire transition from $\lambda = 0$ to $\lambda = 1$, and

$$U_{II}^{(0)} = U_{II}\left(\left\{\mathbf{r}_i^{(0)}\right\}\right). \tag{8}$$

is the value of the potential of interest U_{II} when all the atoms are in equilibrium atomic positions $\mathbf{r}_i^{(0)}$. For the force constants α_i it is convenient to use such values that the rms deviations of atoms from their equilibrium positions at $\lambda = 0$ and $\lambda = 1$ are approximately equal. Using the expression for the rms deviations of atoms in the Einstein harmonic crystal, we get the following condition for the force constants α_i

$$\frac{3k_BT}{\alpha_i} = \left\langle\left(\mathbf{r}_i - \mathbf{r}_i^{(0)}\right)^2\right\rangle_{\lambda=1}. \tag{9}$$

Then the free energy of the Einstein harmonic crystal is

$$F\left(\lambda=0\right)=3k_BT\sum_i\ln\left(\frac{h}{\pi k_BT}\sqrt{\frac{\alpha_i}{m_i}}\right)+U_{II}^{(0)}. \tag{10}$$

Substituting Eq. (10) to Eq. (5) yields

$$\begin{aligned} F\left(\lambda=1\right) &= 3k_BT\sum_i\ln\left(\frac{h}{\pi k_BT}\sqrt{\frac{\alpha_i}{m_i}}\right)+U_{II}^{(0)} \\ &+ \int_0^1 d\lambda\left\langle U_{II}-U_I\right\rangle_\lambda. \end{aligned} \tag{11}$$

Eq. (11) is not referred to any kind of crystal structure, kinds of particles, types of interatomic interaction. The only requirement for modeled system for Eq. (11) to be valid is metastability of the crystal microstructure in the sense that particles oscillate around their equilibrium positions which are steady in time during rather long time period in the frames of the CMD simulation. Eq. (11) can be applied as it is for calculations of free energy values of single component non-defective crystals, multi-component crystal alloys, crystals with defects if those defective micro-structures are stable in time in the timescale of CMD (up to ns), *e.g.* vacancies, vacancy clusters, and dislocations. Particularly, the activation energy for diffusive migration of He atom-vacancy complex is rather high [6], and at the ambient conditions He atoms seating in the fcc lattice of Pu-Ga alloy are motionless in the frames of CMD.

Here we present an example of free energy calculation for the fcc δ-phase Pu-Ga alloy containing 3 $at.$ % Ga and helium atoms in the form of He atom-vacancy complex, *i.e.* helium as substitutional solution, at the ambient conditions. The following CMD simulations were performed with widely-used Modified Embedded Atom Model (MEAM) [27, 28, 29] of interatomic interaction parameterized for fcc plutonium [30], gallium [31], binary fcc Pu-Ga alloys [32, 20], which later was modified to include He atom interactions [7]. In our simulation we used MEAM interatomic potential for binary Pu-Ga alloys with the parameterization from [33] in combination with exp 6 potential for the characterization of He atom interactions with He, Pu, and Ga atoms. The parameterization

of exp 6 potential for the He atom interactions was found in [8] for the best representation of *ab initio* calculation results.

In this example calculation we used Pu-Ga sample $21 \times 21 \times 21$ unit cells $(37,044$ atoms) containing 3 % Ga atoms as disordered substitutional solid solution with periodic boundary conditions in the cartesian directions. 200 He atoms were added to the sample by the substituting of 200 randomly chosen atoms. At first we need to calculate the equilibrium density ρ of the crystal at the conditions of interest. For this end we simulate an NPT-ensemble at the specified parameters $P = 0$ and $T = 300\ K$. The averaging period for the calculation of equilibrium parameters was 1 ns. Prior the averaging of the system characteristics each time the system was relaxed for 100 ps. In the simulations we used combination of Berendsen [34] (initial stages of thermalization) and Nose-Hoover [35, 36] thermostats. During the averaging period we always used Nose-Hoover thermostat because this thermostat allows to simulate canonical ensemble [35, 36, 24], which is critical for the adequate description of phase space occupied by the system at fixed values of volume V and temperature T. The purpose of this initial calculation is to get the equilibrium density ρ (or better to say equilibrium sizes and shape of the system in order to avoid tangential stresses) which will be fixed in all future calculations for the canonical NVT ensemble.

The simulation of the NPT-ensemble is followed by the simulation of canonical NVT-ensemble simulation with the same averaging and thermalization times as for the NPT-ensemble. In this simulation we determine the equilibrium positions of atoms which, in general, in the alloy with the addition of noble gas atoms at finite temperatures may differ from the nodes of the ideal crystal lattice, and calculate the rms deviations of atoms from their equilibrium positions. The calculated equilibrium positions of atoms $\mathbf{r}_i^{(0)}$ will be used to calculate potential U_I (Eq. (7)), and their rms deviations will be used to fix the force constants α_i using Eq. (9). If atoms differ in type and/or atomic positions in the crystal lattice are not equivalent, it is necessary to calculate rms deviations for each type/position of atoms and, accordingly, the appropriate values of α_i.

With the equilibrium positions and rms deviations of atoms calculated for the specified conditions we obtain harmonic approximation (7) for the crystal.

Having the harmonic approximation we can calculate the free energy for the canonical NVT-ensemble of the system of interest. For this end we need to perform a reversible transition from the state of interest to the harmonic crystal and then do the integration in the Eq. (11). To do that we discretely vary λ in a chain of successive simulations to thermalize the system and then calculate time average values of $\langle u_{II} - u_I \rangle_\lambda$ at fixed λ values along the phase trajectories calculated with the interatomic potential (2). The averaging time at each of the λ values was 25 ps with initial thermalization stage after each change of λ for 5 ps. The calculated dependence of average values of $\langle U_{II} - U_I \rangle_\lambda$ on coupling parameter λ along the transition from $\lambda = 1$ to $\lambda = 0$ for Pu-Ga samples with He atoms in the form of single He atom-vacancy complexes is shown in Fig. 1 by diamonds. We verify the correctness of the result by two methods. The first is the check whether inequality (6) is satisfied or not. The second is verification if the transition is reversible. That is, after we have done the transition from $\lambda = 1$ (the crystal with the interatomic potential of interest) to $\lambda = 0$ (the Einstein harmonic crystal), we can do the reverse transition from $\lambda = 0$ to $\lambda = 1$ using the same values of λ in reverse order. If the resulted values of $\langle u_{II} - u_I \rangle_\lambda$ reasonably agree with those obtained in the direct transition for all values of λ, we can claim that the transition is quasi-equilibrium and reversible, and the integral in Eq. (11) is estimated quite accurately. If not, the transition is not equilibrium and it is necessary either to make the steps of λ smaller, and/or to increase times for relaxation and calculation of time averages at each λ. Figure 1 shows time average potential energy $\langle U_{II} - U_I \rangle_\lambda$ versus λ obtained in successive chain of simulations from $\lambda = 1$ to $\lambda = 0$ ($\diamond$) and back ($\times$). The results are seen to agree well for all values of λ and satisfy inequality (6), *i.e.*, the transition is reversible and quasi-equilibrium, and the dependence can be used for calculation of the integral in Eq. (11).

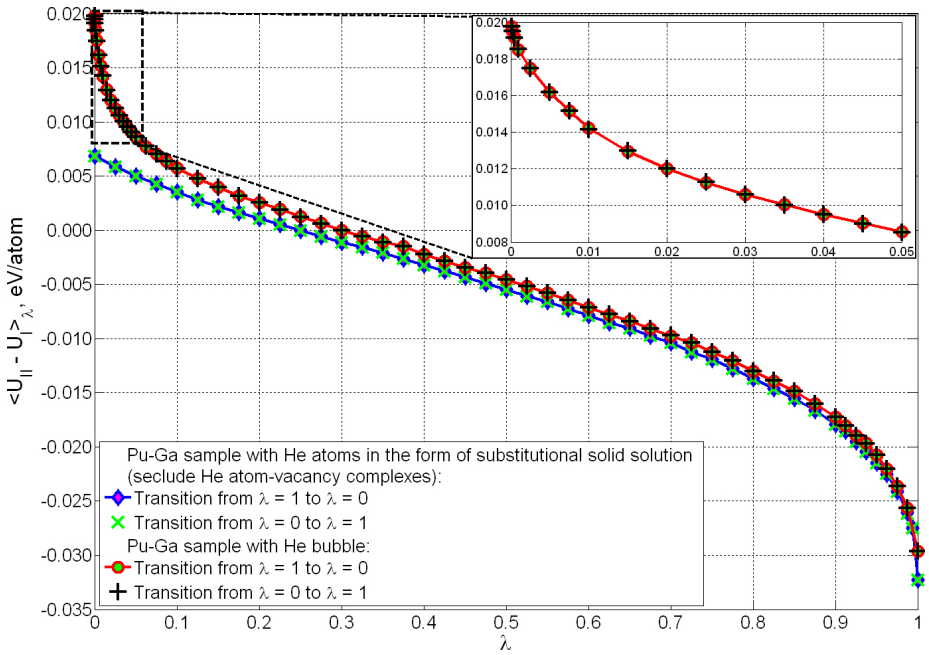

Figure 1: (Color online) Typical dependence of average values of $\langle U_{II} - U_I \rangle_\lambda$ on coupling parameter λ along direct (from $\lambda = 1$ to $\lambda = 0$) and reverse (from $\lambda = 0$ to $\lambda = 1$) transitions obtained in numerical simulations for Pu-Ga samples with He atoms in the form of single He atom-vacancy complexes ($\diamond$ and $\times$) and He bubbles ($\circ$ and $+$). Symbols correspond to the values of coupling parameter λ for which we performed the averaging in a series of successive calculations discretely changing λ from 1 to 0 and back.

2.3. Free Energy of Pu-Ga Alloys with He Bubbles

In the previous example, where He atoms were dissolved in the lattice, they are almost motionless in terms of diffusive migration trough the lattice at times available for CMD, and Helmholtz free energy of such systems can be calculated with an approximation of the Einstein harmonic crystal in the high temperature limit. On the other hand, in the fcc Pu-Ga alloys with He-bubbles, helium is in liquid state in the bubbles. He atoms in the bubble moves freely inside the bubble without steady equilibrium positions, while they are restricted by the surrounding lattice to leave the bubbles and do not dissolve into the lattice in CMD simulations at the ambient conditions [8]. Thus, the application of TIM for the systems containing He bubbles requires a technique which would be capable of calculating free energy for crystal and liquid restricted in a certain volume simultaneously.

TIM is defined by the model potential U_I which is required to provide for a reversible quasi-equilibrium transition from the state of interest $\lambda = 1$ to the reference state $\lambda = 0$, where one can anyhow (best of all, analytically) calculate free energy. The potential U_I for the systems with He bubbles was constructed in the following way. As mentioned above, the system with a bubble combines a Pu-Ga crystal (probably, with addition of He atoms as substitutional lattice atoms) and a liquid of He atoms in a quasi-spherical bubble. For atoms which form the crystal, it is natural to use an approximation of Einstein harmonic crystal. For He atoms in the bubble, we need a potential that would keep them in a liquid state but would not allow the bubble to disperse during the transition from $\lambda = 1$ to $\lambda = 0$. That is why we propose using an approximation of ideal gas in a smooth potential well with a rather steep wall (to effectively keep He atoms in the bubble), which has a width corresponding to the equilibrium size of the bubble and is centered at the center of the bubble in equilibrium. So, we calculate the free energy of systems with He bubbles using the model potential

U_I in the form

$$\begin{aligned} U_I(\mathbf{r}_i) &= \left\{ \sum_{crystal} \frac{\alpha_i}{2} \left(\mathbf{r}_i - \mathbf{r}_i^{(0)} \right)^2 + U_{II\ crystal}^{(0)} \right\} \\ &+ \left\{ \sum_{bubble} U_0 \left(\frac{|\mathbf{r}_i - \mathbf{r}_c|}{R} \right)^n \right\}, \end{aligned} \tag{12}$$

where $\mathbf{r}_c$ is the bubble center, R - its equilibrium radius, n - arbitrary power, and U_0 - the energy constant of the potential. The values of n and U_0 should be chosen such that smooth potential well would be rather flat within the bubble (for $|\mathbf{r} - \mathbf{r}_c| < R$) and would have steep wall at $|\mathbf{r} - \mathbf{r}_c| > R$ restricting He atoms from the escape from the bubble. In our CMD simulations we used $n = 10$ and $U_0 = 0.1\ eV$ For this potential we can analytically compute the statistical integral and calculate free energy. Specifically, for the free energy of ideal gas of He atoms in the potential well, we obtain

$$\begin{aligned} F_{bubble}(\lambda = 0) &= k_B T \ln(\Gamma(N_b + 1)) \\ &- 3 N_b k_B T \ln \left(\frac{2R}{n \Lambda_T} \Gamma\left(\frac{1}{n}\right) \left(\frac{k_B T}{U_0}\right)^{\frac{1}{n}} \right), \end{aligned} \tag{13}$$

where N_b is number of He atoms in the bubble, factor $\Gamma(N_b + 1) = N_b!$ is due to the equivalence of the particles in the bubble (exchange of the particles does not change a microstate). Using Eqs. (11) and (13) one can calculate free energy of the reference state for the Pu-Ga system with He bubble.

One more peculiarity of free energy calculation for Pu-Ga systems with He bubble comes from the fact that the potential which models the interaction of He atoms with other components - $\exp 6$ - is singular at $r = 0$, moreover, it is negative as r approaches 0 (dashed lines in Fig. 2). This means that in TIM over the transition from state $\lambda = 1$ to state $\lambda = 0$, the He atoms which overcome the repulsion barrier will attract one another. This will give a non-physical segregation of He atoms in the bubble which won't dissolve in the reverse transition. To avoid this we need to modify the potential in such a way as to make it non-negative and non-singular at $r \to 0$, but do not change the equilibrium properties of the He bubble in the crystal matrix for the usual CMD

calculation. For this end we replace the original exp 6 potential by a potential which equals exp 6 at $r \geq r_0$ (in the described calculations r_0 was taken to be 0.15 nm) and is the straight line $U(r) = (dU_{\exp -6}/dr)_{r=r_0}(r - r_0) + U_{\exp -6}(r_0)$ at $r < 0$. We thus obtain a smooth, everywhere continuous potential which is equal to the original exp 6 at $r \geq r_0$ and non-negative as $r \to 0$ (solid lines in Fig. 2).

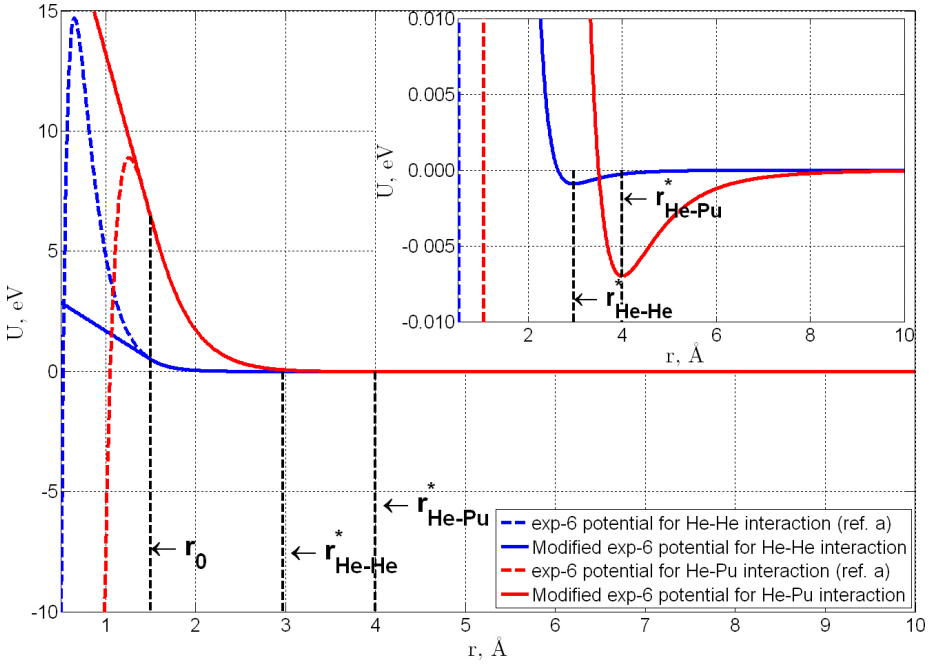

Figure 2: (Color online) Modification of exp 6 potential for He-He and He-Pu interactions. Solid lines - original exp 6 potentials from ref. a [8], dashed lines - modification of the exp 6 potentials in order to avoid negative singularity in the vicinity of $r \to 0$.

The free energy calculations for Pu-Ga systems with He bubbles is performed in three steps in the manner similar to that in Subsection 2.2. The first step is the simulation of the NPT-ensemble to relax the system at specified conditions and find its equilibrium size. Then, with the obtained size fixed, we simulate the canonical NVT-ensemble to get equilibrium positions and rms deviations (force constants) for atoms in the crystal, and the equilibrium size and center of the bubble which are used for model potential (12). Then we choose values for

U_0 and n. The latter should be large enough to make the wall of the potential rather steep at $|\mathbf{r} - \mathbf{r}_c| > R$ and the bottom "flat" (in our calculations, $n = 10$). After that we perform the quasi-equilibrium transition from the state of interest ($\lambda = 1$) to the reference state ($\lambda = 0$) in the same manner as we did for the Pu-Ga crystal with dissolved helium. In Fig. 1 one can see the dependence of average potential energy $\langle U_{II} - U_I \rangle_\lambda$ on the coupling parameter λ in the successive quasi-equilibrium transition from $\lambda = 1$ to $\lambda = 0$ shown by circles. The curve is seen to combine the features of the λ dependent $\langle U_{II} - U_I \rangle_\lambda$ obtained for the crystal ($\diamond$'s and $\times$'s in Fig. 1) with rapid increase as λ approaches 0 that corresponds to arbitrary approach of He atoms inside the potential well when the repulsion of the $\exp 6$ potential "turned off" by decreasing λ. The implemented reverse transition from $\lambda = 0$ to $\lambda = 1$ showed the resulted values of $\langle U_{II} - U_I \rangle_\lambda$ (shown by + in Fig. 1) to agree well with the values obtained in the direct transition from $\lambda = 1$ to $\lambda = 0$ for all λ's. As one can see in Fig. 1 the dependence of $\langle U_{II} - U_I \rangle_\lambda$ on λ satisfies Inq. (6). Thus, we can assert that the transition is reversible and quasi-equilibrium and can be used to calculate the free energy value using Eqs. (5),(10), and (13).

3. Solubility of He in Pu-Ga Alloys

The first CMD calculations of free energies using TIM we performed to verify helium solubility in δ-phase fcc Pu-Ga alloys at the ambient conditions. We used systems of two kinds which were identical in composition and in the number of atoms, but varied by micro-configuration. We generated a set of fcc Pu-Ga samples with 4.7 $at.$ % of gallium as disordered substitutional solid solution $21 \times 21 \times 21$ unit cells (box size is ~ 10 nm - $37,044$ atoms) and added 50 He atoms in two different ways. The first is He atoms in the form of He atoms-vacancy complexes when we simply replaced by He randomly chosen 50 lattice atoms. The second is He bubble with He concentration 1 atom per vacant site when we replaced 50 lattice atoms in the center of the sample by He atoms. Thus, the systems with distributed helium and helium in the form of bubble consist of

identical number of particles and can be interpreted as rearrangements of Pu, Ga and He inside the box at the same conditions, and their internal and free energies can be directly compared in order to make conclusions about energetic and thermodynamic preference of those micro-configurations at the conditions of interest. In order to have better statistics we generated ten samples of each kind varying distribution of Ga and He atoms inside the samples. Obtained values of internal and free energies were averaged over the samples.

The procedure of free energy calculations using TIM for both kinds of systems is described in details in Subsections 2.2 and 2.3. The results of the internal and free energies comparison are the following: the configuration with a He bubble of 50 atoms with the concentration 1 He atom per vacant site was found about 19 eV (0.38 eV per atom) of internal energy and about 24 eV (0.48 eV per atom) of free energy more favorable than the configuration with uniformly distributed He atom-vacancy complexes. Comparing this energies with $k_BT = 0.026\ eV$ this outcome allows an unambiguous conclusion that, in accord with CMD simulations with MEAM+exp 6 potential being used, under the ambient conditions He atoms do not dissolve in Pu-Ga alloys and do not form a disordered substitution solution. Even low concentration and small size He bubbles compared to those reported in [14] are preferable from the thermodynamics than the uniformly distributed in the lattice He atom-vacancy complexes.

The next series of calculations we performed to investigate interaction of single He atom-vacancy complexes with He bubbles of various size and He concentration. Again the CMD calculations of free energies using TIM were done for two kinds of systems which were identical in composition and in the number of atoms but varied by micro-configuration, and then their internal and free energies were compared to assess thermodynamic preference. As initial step we generated a set of fcc Pu-Ga samples with 3 $at.$ % of gallium as disordered substitutional solid solution $19 \times 19 \times 19$ unit cells (box size is $\sim 9\ nm$ - $27,436$ atoms), then we took away atoms inside spheres of various radii from 0.8 nm to 1.5 nm in the center of the samples and filled those voids with He atoms with

various concentrations 1, 2, 2.5, 3, 4 He atoms per vacant site (see Fig. 3a). In order to have better statistics we generated ten samples of each combination of radius and He atom concentrations in the bubbles varying distribution of Ga atoms in the samples.

The initial samples were thermalized at the ambient conditions in NPT-ensemble CMD simulations with periodic boundary conditions for rather long time for CMD simulations ($\sim 2\ ns$). The long-time CMD simulation of equilibration of He atoms in the fcc lattice of Pu-Ga alloys is crucial, since, as it was demonstrated in [8], if we stop the simulation at $t \sim 100\ ps$ we can come to erroneous conclusion that He bubbles are unstable in the frames of CMD with MEAM potential [7] based on the damage of the fcc lattice around the bubbles seen for that instance of time. However, if we continue the simulation up to a couple of ns the crystal lattice around the bubbles recovers after damage, and He bubbles obtain their equilibrium size and shape. Note, that effective pressure in He bubbles is estimated to be rather high ($\sim 3\ GPa$) [37], that manifests itself as an expansion of the bubbles compared to the initial taken away sphere of Pu or Ga atoms, and this expansion is higher for the higher He concentrations in the bubbles.

To the thermalized systems with He bubbles of various sizes and He concentrations we added 50 He atoms in two different ways. The first is when we added 50 He atoms in the form of He atom-vacancy complexes located away from the initial bubbles. For that we added 50 He atoms (shown by magenta dots in Fig. 3b) to the systems replacing 50 Pu or Ga atoms outside sphere 5 nm in diameter centered in the center of the initial He bubble (shown by gray sphere in Fig. 3b). The second way is when we added 50 He atoms directly to the initial bubbles by replacing of 50 Pu or Ga atoms edging the initial He bubble (see Fig. 3c). The resultant micro-configurations again were thermalized in NPT-ensemble CMD simulations for $\sim 1\ ns$.

For the systems with increased in size He bubbles and with He bubbles and 50 additional He atoms distributed in the bulk of the samples we performed the calculations of absolute values of free Helmholtz and internal energies and

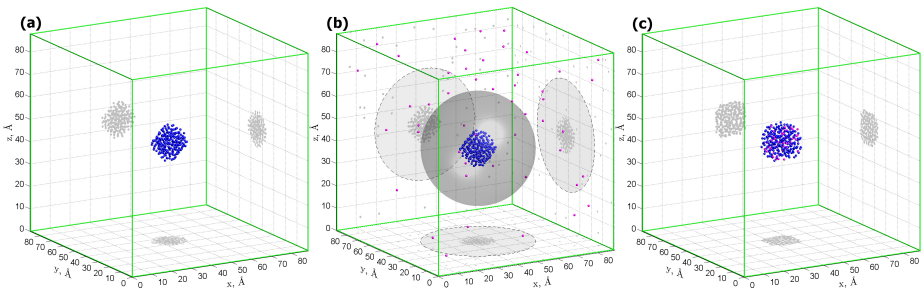

Figure 3: (Color online) System configurations for investigation of solubility of helium in fcc lattice of Pu-Ga alloys at the ambient conditions (Only He atoms are shown). a - initial system with He bubble made by removing of Pu or Ga atoms inside sphere of certain radius and replacing them by He atoms (shown by blue dots) with certain He atom per vacant site ratio, b - 50 He atoms (magenta dots) have been added to the system by replacing 50 Pu or Ga atoms outside sphere 5 nm in diameter centered in the center of the initial He bubble (gray sphere), c - 50 He atoms (magenta dots) have been added to the system by replacing of 50 Pu or Ga atoms on the surface of the initial He bubble.

compared them. In Fig. 4 the results of such comparison, namely, the difference between the internal (Fig. 4a) and free (Fig. 4b) energies of the systems with the increased bubble (Fig. 3c) and the systems with the bubble and distributed He (Fig. 3b) are presented. In other words in Fig. 4 the internal and free energy profit resulting from the joining of 50 He atom-vacancy complexes to He bubbles of certain size and He concentration (shown by black points in Fig. 4) is shown.

The first one needs to notice in Fig. 4 is that the both the internal energy difference (Fig. 4a) and free energy difference (Fig. 4b) are negative in the entire ranges of He concentrations and bubble sizes. That is for all the sizes of the bubbles and He concentration both the internal and free energies of the systems gain from the joining of 50 He atom-vacancy complexes to any of the bubbles. So, the increased size He bubble configuration is more preferable than the bubble with distributed He atoms in both the energy and that is more important in thermodynamic sense. This means that if He atom-vacancy complexes can diffusively migrate in the lattice at the ambient conditions they would "prefer" to join any of the He bubbles rather then stay as singe substitutional He atom in the lattice. In other words, under the ambient conditions He atoms do not

dissolve in Pu-Ga alloys.

The second important feature in Fig. 4 is dramatic difference in the character of the internal energy surface and that of free energy. That is why it is absolutely necessary to investigate the free energy surfaces rather than the internal energy if one needs to study relative thermodynamic stability at finite temperatures especially for the mixes of the crystal structure and the liquid in the bubble. The main result we obtained is that the surface of free energy difference (free energy profit from the joining of 50 atoms to the initial He bubble) has minimum in the point $C \approx 2.7$ and $R \approx 1.1\ nm$. This can be interpreted in the following way. If 50 single He atoms distributed in the bulk of a sample as substitution atoms would join to He bubble of such size and He concentration it would result in the highest decrease of free Helmholtz energy of the system which is the most preferable from the thermodynamic point of view. Thus the values of $C = 2.7$ and $R = 1.1\ nm$ can be treated as estimates for the thermodynamically equilibrium parameters of He bubbles in the Pu-3 $at.$ % Ga fcc alloy at the ambient conditions. The calculated equilibrium size is slightly higher than the experimentally observed value of average He bubble radius which is of the order $0.7-0.8\ nm$ [14], while the obtained equilibrium He concentration value $C = 2.7$ agrees well with the experimentally observed values of order $2-3$ He atoms per vacant site [14].

4. Equilibrium size of He bubbles

In the present section we introduce a way to estimate thermodynamically equilibrium size of He bubble with fixed He concentration in the lattice of Pu-Ga alloy. In the following we fixed He concentration to be $C = 2.7$ that agrees with the experimentally observed $2-3$ He atoms per vacant site [14]. In order to obtain dependence of Helmholtz free energy of the system on the size of He bubbles we need to perform a series of CMD calculations to get free energies of the systems which were identical in composition and in the number of atoms but varied by micro-configuration increasing the size of the bubble keeping He

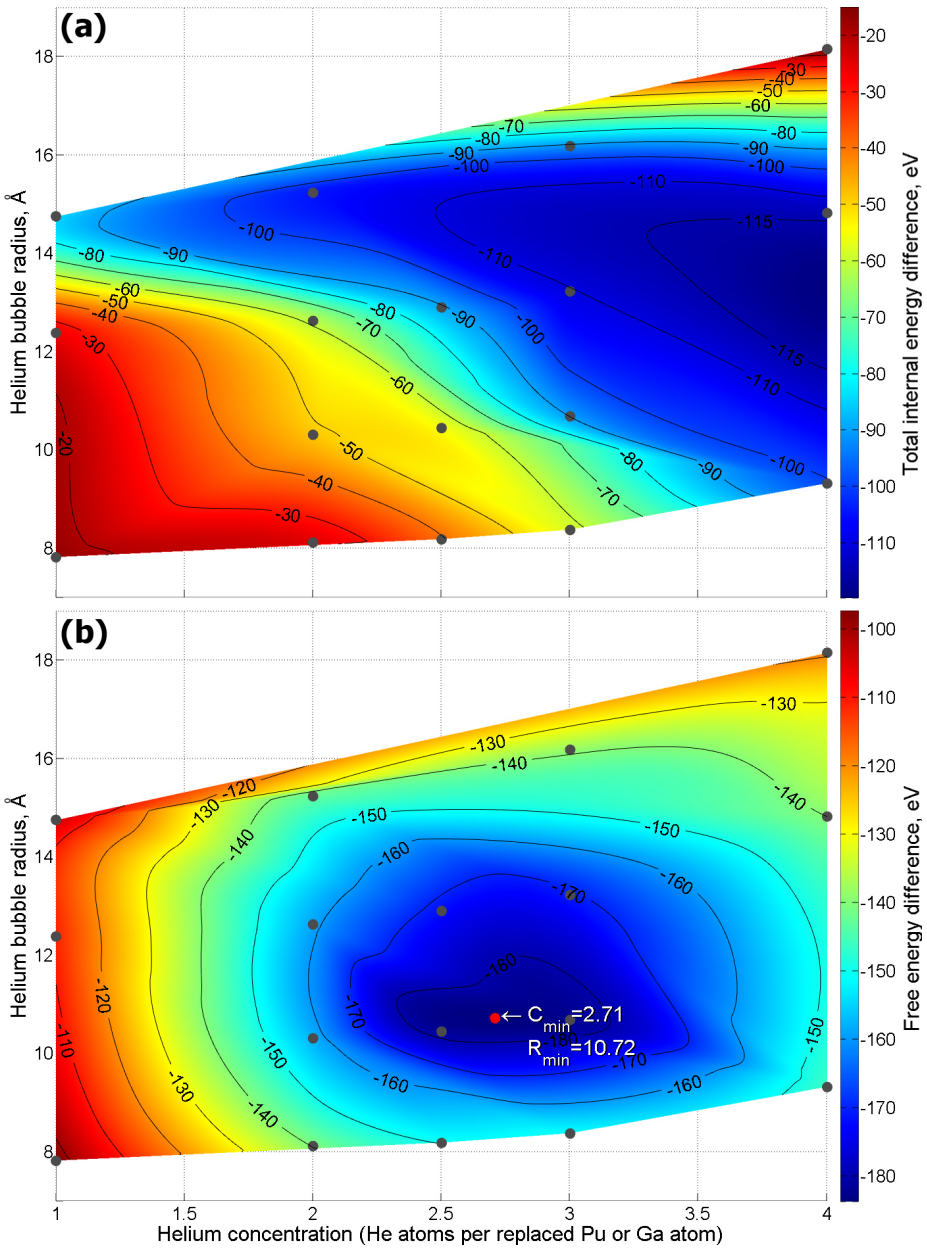

Figure 4: (Color online) (a) - internal and (b) - free energy differences of the systems with all He atoms placed in the bubbles and systems with He bubbles and distributed away from the bubbles He atoms as functions of helium concentration (number of He atoms per vacant site) and the size of initial bubbles. Calculations of the internal and free energy differences were performed for the parameters shown by the black points, and color surfaces with isolines are 2D spline interpolations of the values at the black points. Red point marked by white arrow corresponds to the minimal value on the surface.

concentration constant. That would require TIM free energy calculation with rather big samples containing one bubble the size of which will increase, small bubbles or distributed He atoms as the source of He atoms for the main bubble growth, and non-defective crystal which fraction in the entire sample will grow with increasing size of the bubble. The CMD simulations with big samples with the sampling for better statistics for rather long times would require vast computational resources and more importantly huge computational time.

On the other hand, free energy is an additive function meaning that the free energy of the entire system is equal to the sum of free energies of its parts at the same conditions. In order to check if the free energies values calculated in CMD simulations using TIM satisfy the additivity rule we performed series of simulations in the following manner. We generated two sets of Pu-3 *at.* % Ga samples $21 \times 21 \times 21$ and $42 \times 21 \times 21$ unit cells (10 samples of each kind for statistics) and thermalized them in NPT-ensemble CMD simulations at the ambient conditions. Then we calculated free energy values for non-defective samples of both sizes. The result is that average free energy of the bigger samples within the confidence band is twice the average free energy of the smaller ones. As the next step we added to both kinds of the samples He bubbles containing 54 He atoms with concentration $C = 2.7$, and calculated their free energies. Average free energy of $42 \times 21 \times 21$ samples with one He bubble of 54 atoms within the confidence band coincides with sum of average free energy of $21 \times 21 \times 21$ samples without helium and average free energy of $21 \times 21 \times 21$ samples with the 54 atoms He bubble. Than we added to the bigger samples one more He bubble of the same size and He concentration but far apart from the initial bubble and calculated their free energies. We got that average free energy of the bigger system with two bubbles is twice the free energy of smaller systems with one bubble in each. The final check of the free energy additivity we performed for the $42 \times 21 \times 21$ system with two bubbles. We increased the size of one of the bubbles by 54 atoms keeping He concentration the same. Thus, the bigger samples contained 108 and 54 atoms He bubbles. In order to have the similar constituent smaller system we made in the $21 \times 21 \times 21$ samples He bubbles with

108 atoms He concentration $C = 2.7$ as well. The comparison of average free energy of bigger system with two 108 and 54 atoms He bubbles and the sum of average free energy of smaller systems with the He bubbles with 108 and 54 atoms and all the previous tests allow to conclude that the additivity rule for Helmholtz free energy values in our CMD simulations is fulfilled.

The confirmed additivity of free energy values obtained in our CMD calculations using TIM allows us instead of time and computational resources consuming CMD simulations with huge number of particles to perform the free energy calculations by parts. We calculated the free energies of Pu-3 $at.$ % Ga samples $21 \times 21 \times 21$ without He, Pu-3 $at.$ % Ga samples $21 \times 21 \times 21$ containing He bubble of 54 atoms with concentration $C = 2.7$ (this bubble serves as the source of growth of the "main" bubble), and Pu-3 $at.$ % Ga samples $21 \times 21 \times 21$ containing He bubbles with 108, 162, 216, 270, 324, 378, and 432 atoms with concentration $C = 2.7$. Again for the statistic purposes we generated and thermalized 20 samples identical in composition and in the number of atoms, but varied by distribution of Ga atoms in the lattice. In principle, we could do the finer step in the bubble size, but that would require to increase significantly the amount of CMD simulations but would not change the character of the result.

One can imagine a system that consists of K subsystem of $21 \times 21 \times 21$ with one He bubble of 54 atoms (the first row in Fig. 5). Lets denote the free energy of such subsystem as F_{54}. Than the free energy of the whole system is $F = K \cdot F_{54}$. Now let replace one of the subsystems by a subsystem without helium (the free energy of such subsystem - F_0). In order to keep the number of He atoms in the entire system constant we increase the number of He atoms in one of the bubbles by 54 atoms (the free energy of such subsystem - F_{108}). Than the free energy gain from the coalescence of two of the 54 atoms He bubbles (the second row in Fig. 5) is $\Delta F_{108} = F_{108} + F_0 - 2F_{54}$. Than we increase the size of the "main" bubble by 54 He atoms to 162 and in accordance replace one of the subsystems with 54 atoms He bubble by the non-defective crystal. Then the free energy gain from the coalescence of three of the 54 atoms He bubbles (the third row in Fig. 5) is $\Delta F_{162} = F_{162} + 2F_0 - 3F_{54}$. The next bubble size

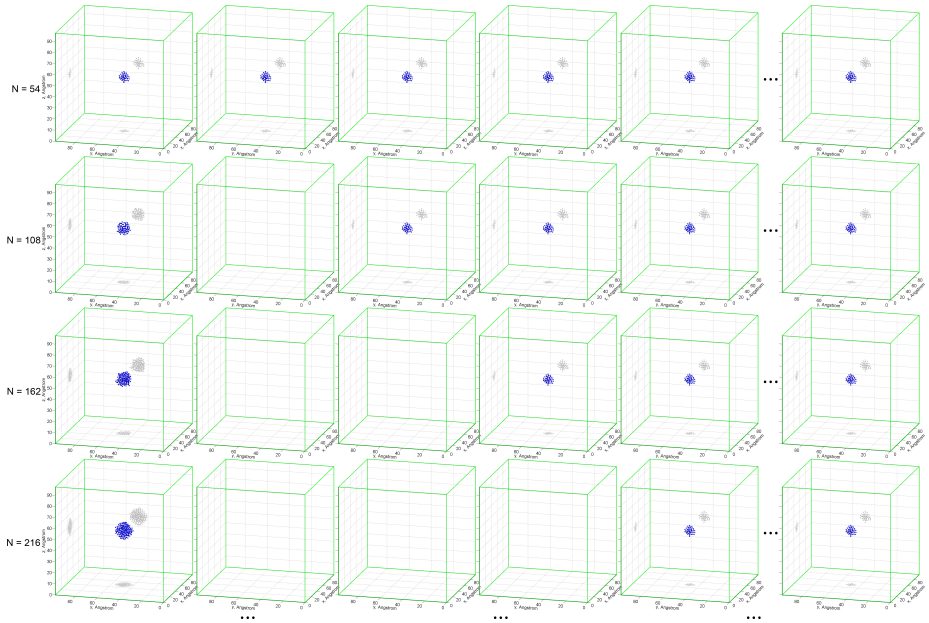

Figure 5: (Color online) Illustration to the calculations of He bubble growth effect on free energy of the system at the ambient conditions (Only He atoms are shown). In the first row the system consists of subsystems $21 \times 21 \times 21$ unit cells with He bubble of 54 atoms with He concentration $C = 2.7$. In the second row the size of the first He bubble is increased by 54 atoms. In order to keep the number of particles and the composition in the entire sample constant one of the subsystems with 54 atoms He bubble by non-defective crystal subsystem. In the third row the size of the first He bubble again is increased by 54 atoms, and one more subsystem with 54 atoms He bubble is replaced by the non-defective crystal subsystem, and so on. As the result all the systems in the rows consists of the same number of particles and have the same composition but various micro-configurations. Thus, their internal and free energy values can be compared directly.

free energy gain is $\Delta F_{216} = F_{216} + 3F_0 - 4F_{54}$ and so on.

In Fig. 6a the results of described above calculations for the internal (red circles) and free (blue squares) energies are presented. The values in Fig. 6a have the meaning of the internal and free energy gains resultant from the coalescence of 54 atoms He bubbles while the concentration in the bubbles is kept constant $C = 2.7$. The negative values of the internal and free energy changes with the growth of the "main" He bubble means that the growth of the bubble with He concentration $C = 2.7$ through the mechanism of coalescence of smaller (54 He atoms) bubbles is energetically and thermodynamically profitable. Red solid and blue dashed lines in Fig. 6a are polynomial regressions of the corresponding values of the relative internal and free energies respectively.

If we consider the He bubble growing in our CMD simulations as a system at constant pressure and temperature that can exchange particles (He atoms) with the surroundings then the condition for the thermodynamic equilibrium of such system is the minimum of the chemical potential μ [38, 39]. The chemical potential μ can be found as

$$\mu = \left(\frac{\partial G}{\partial N}\right)_{P,T}, \tag{14}$$

where G - Gibbs thermodynamic potential, and N number of particles in the system. Since, Gibbs potential is $G = F + PV$, and the pressure P is equal zero in our simulations then

$$\mu = \left(\frac{\partial F}{\partial N}\right)_{P=0,T}. \tag{15}$$

If we differentiate the polynomial approximations in Fig. 6a with respect to N we get the dependence presented in Fig. 6b. Ones again we would like to draw attention of readers to the significant difference in the behavior of the internal and free energies at the finite temperatures and emphasize that in order to determine relative stability of micro-configurations at finite temperatures it is insufficient to compare internal energies. One must make conclusions about thermodynamic preference of microstates based on the comparison of the thermodynamic potentials. The blue dashed line in Fig. 14b have the meaning of

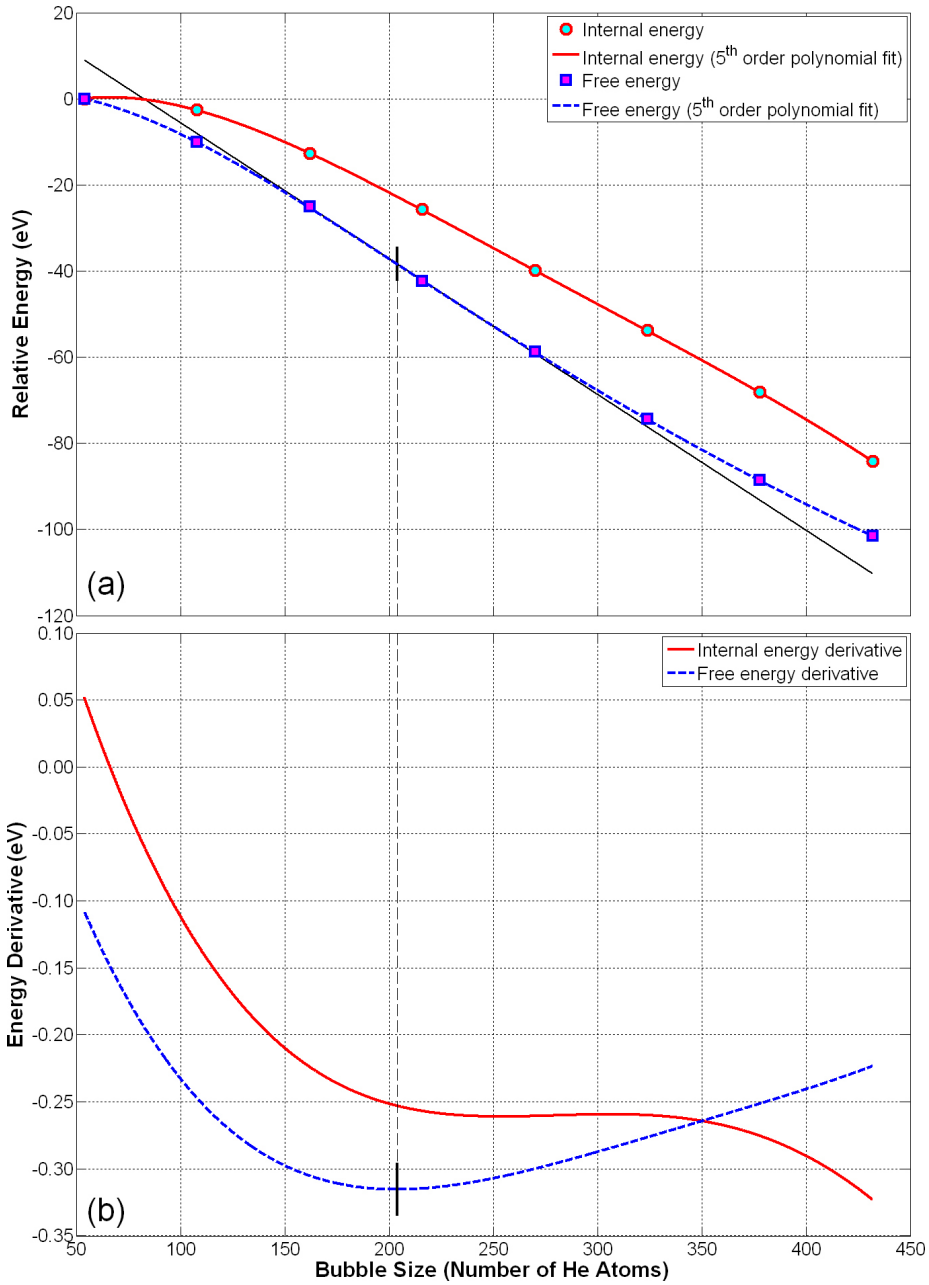

Figure 6: (Color online) a - relative internal and free energies as functions of number of particles N in He bubble with He concentration $C = 2.7$, b - derivatives of the internal and free energies with respect to N.

effective chemical potential of the He atoms in the bubble with He concentration $C = 2.7$ which growths by the mechanism of coalescence of 54 atoms He bubbles of the same concentration. The chemical potential dependence on N has minimum at $N \approx 205$ and the minimum chemical potential value $\mu_0 = -0.315\ eV$. This means that in the frames of CMD with MEAM+exp 6 interatomic potential for Pu-Ga-He interactions [8] taking into account only one mechanism of growth of He bubbles (coalescence of smaller bubbles) with fixed concentration $C = 2.7$ at the ambient conditions there is thermodynamically equilibrium size of He bubble $N = 205$.

In Fig. 7 calculated in NPT-ensemble CMD simulations dependence of equilibrium radius of He bubbles with the fixed He concentration $C = 2.7$ on the number of He atoms in the bubbles is shown. Diamonds in Fig. 7 represent values of equilibrium He bubble radii obtained for individual samples, circles with the error margins are the mean values with the standard deviations for the corresponding number of He atoms N, solid blue line represents least-squares regression of the diamonds, and red dashed line is the radius of a sphere with the volume equal to the total volume occupied by the replaced atoms in the initial non-defective lattice. As one can see for all the sizes of the He bubbles presented in Fig. 7 with the fixed He concentration $C = 2.7$ the bubbles expand compared to the initial lattice void volume and suppress the surrounding fcc lattice due to quite high effective pressure inside the bubbles.

If we combine the dependence of chemical potential μ on the number of particles N (see Fig. 6b) with the dependence of the equilibrium He bubble radius R on the number of particles N (see Fig. 7), we get $\mu(R)$ and can construct distribution function $f(R)$ of He bubbles with the fixed concentration $C = 2.7$. According to classical thermodynamics the distribution function will be proportional to the Boltzman factor. Thus, up to normalization factor

$$f(R) \sim \exp\left(-\frac{\mu(R) - \mu_0}{k_B T}\right). \tag{16}$$

The distribution function given by Eq. (16) calculated using the data from Figs. 6,7 is presented in Fig. 8 by blue dashed line in comparison with experi-

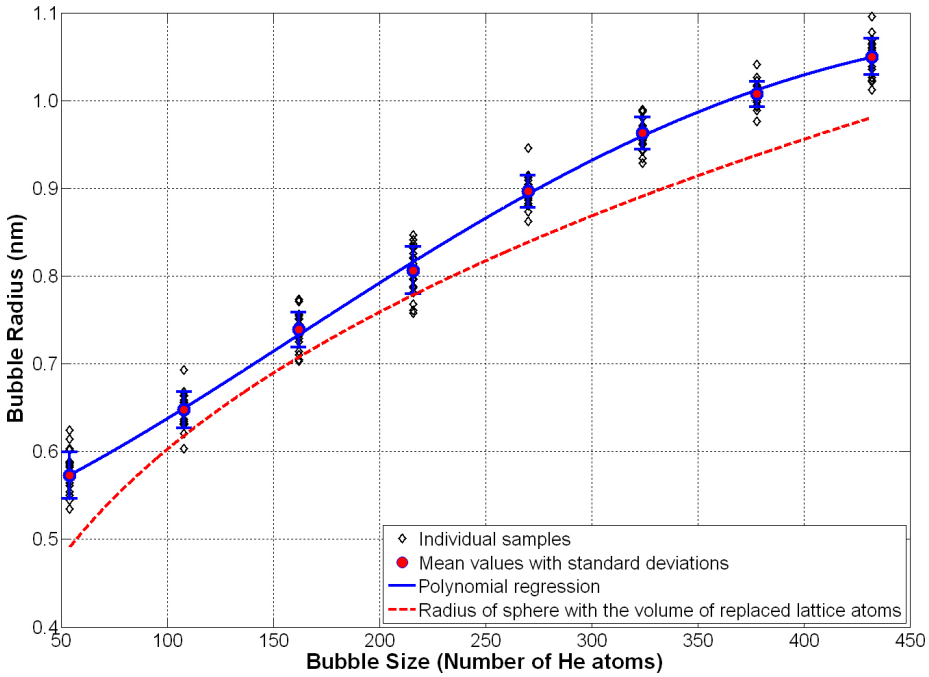

Figure 7: (Color online) Dependence of equilibrium radius of He bubbles with the fixed He concentration $C = 2.7$ on the number of He atoms in the bubbles.

mentally observed distribution function of He bubble radii [14] shown by bars. The bar plot in Fig. 8 is a combined histograms presented in Fig. 4 of [14] obtained for 26, 35, 36, and 42 year-old material and then divided by the maximal number of counts.

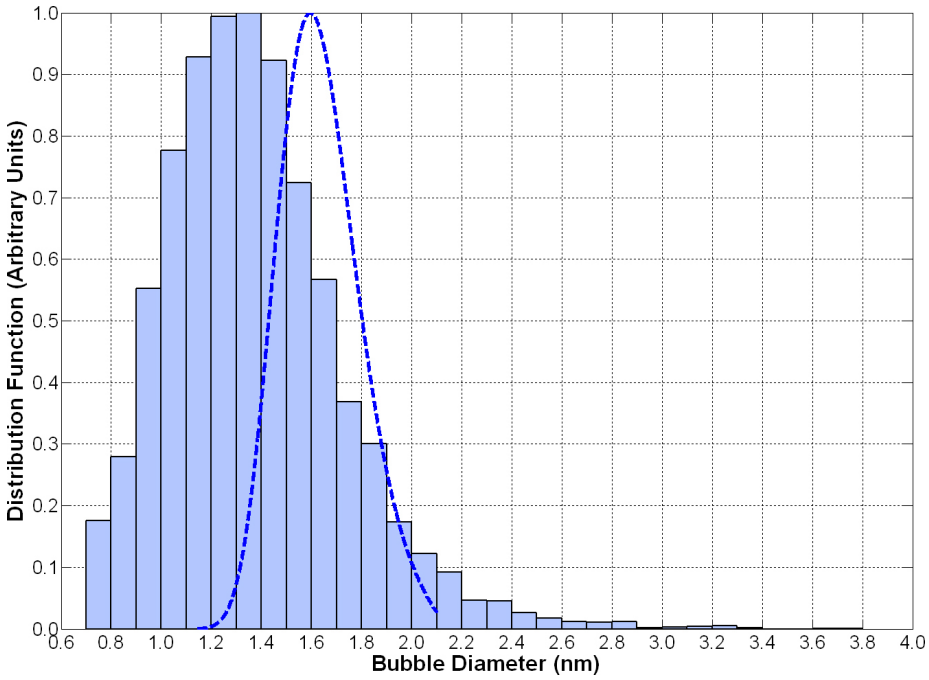

Figure 8: (Color online) Calculated in the present paper helium bubble distribution function with the fixed He concentration $C = 2.7$ (blue dashed line) in comparison with experimentally observed distribution function on 26, 35, 36, and 42 year-old material [14].

As one can see in Fig. 8 the overall characters of the calculated in the frames of CMD and obtained by TEM [14] He bubble radius distribution functions are quite similar. Although there are two major discrepancies between them, namely, the location of maximum ($\sim$ 1.6 nm in CMD dependence) and ($\sim$ 1.4 nm in the experiment) and the width of the distributions - experimental distribution is much wider than the calculated one. We can propose a variety of plausible explanations for these discrepancies.

First of all the result obtained in CMD simulations are determined totally

by the used model of interatomic interaction. MEAM potential for Pu-Ga alloys was parameterized for the certain conditions, and in spite of the fact that it has shown oneself to provide good results for the modeling of the fcc Pu-Ga alloys in a variety of conditions, it does not necessarily describe the defective Pu-Ga alloys with He in it with the same accuracy. On the other hand, the qualitative replication of the experimental distribution function by the calculated one allows to claim that the used MEAM+exp 6 interatomic potential captures the physics of the interaction of He atoms with Pu-Ga fcc lattice qualitatively correct.

The second plausible factor that affects the equilibrium parameters of the He bubbles which requires deeper understanding is possible influence of the alloy composition (local Ga concentration). If for example the equilibrium radius of He bubbles depends on the Ga concentration then it would vary not only from sample to sample with different average Ga content but also from region to region inside the same sample, since Ga content is not uniform inside δ-phase Pu-Ga crystal grains (see for example [40]). If this is the case then it would cause broadening of the distribution. For that it would be useful to repeat the presented CMD calculations for other Ga content of the alloy.

Another factor providing the discrepancies between the experimental and calculated distributions is that in our CMD simulations we used the fixed He atom per vacant site ratio $C = 2.7$. In reality there is a distribution of He bubbles with respect to the He concentration in them determined by the thermodynamics as well. According to the estimate of [14] the average He concentration in the experiments is order of $2 - 3$. The distribution of He bubbles along He concentrations also results in the broadening of the overall distribution.

Finally, in our simulation we considered only one mechanism of the He bubble growth, the coalescence of smaller bubbles with the same fixed He concentration. Of course at the finite temperatures it is not the only mechanism: there are bubbles with different He concentrations and He atom-vacancy complexes produced as the result of α-decay. If those can migrate in the Pu-Ga lattice at the ambient temperatures, this would cause modification of the He bubble radius distribution function, its broadening and possible shift of its maximum.

5. Conclusion

Within the scope of a theoretical study in the frames of CMD into the response of δ-phase Pu-Ga alloys on self-irradiation we have investigated the behavior of He atoms in the fcc lattice of Pu-Ga alloy at the ambient conditions. Because of the low mobility (from standpoint CMD) of He atoms in the Pu-Ga alloy lattice their dynamics cannot be tracked in direct CMD simulations. Instead, we used the Helmholtz free energy function to investigate the equilibrium thermodynamics of metastable states (micro-configurations) in an initially perfect Pu-Ga crystal and perfect crystals with introduced He atoms in different configurations.

Helmholtz free energy of metastable micro-configurations was calculated through thermodynamic integration method (TIM) [22, 23, 24] which was shown to be effective, accurate and thermodynamically consistent through a set of numerical tests. TIM was used to calculate the free energy of the fcc δ-phase Pu-Ga alloy with distributed He atoms as disordered substitutional atoms and with He bubbles of different sizes with various He concentrations (number of He atoms per vacant site) in it. Based on the resulted absolute values of free energy, we drew inferences about the relative thermodynamic stability of different micro-configurations at the ambient conditions, specifically:

1) CMD calculations of solubility of He atoms in the fcc lattice of δ-phase Pu-Ga alloys at the ambient conditions were carried out and it was found in the simulations that for all the parameters of He bubbles used (radius of the bubbles and He atom concentration) the helium bubbles does not dissolve in the matrix of fcc PuGa alloys. From the standpoint of thermodynamics the He atom-vacancy complexes produced as the result of α-decay of ^{239}Pu during diffusive motion inside the lattice should join when meet each other and form the bubbles.

2) A series of CMD calculations using TIM were carried out in order to investigate possible causes stopping He bubbles in the fcc Pu-Ga alloys from continuous growing. It was demonstrated that free Helmholtz energy surface has

minimum for the bubbles of the radius $R = 1.1\ nm$ and $C = 2.7$ helium atoms per vacant site which is close to experimentally observed with TEM average equilibrium parameters of He bubbles in naturally aged material $R = 0.7\ nm$ and $C = 2 - 3$ He atoms per vacant site[14].

3) If we fix He concentration in the bubbles $C = 2.7$ than estimated thermodynamically equilibrium size of He bubbles is ~ 205 He atoms or the radius $R \approx 0.8\ nm$, while experimentally observed result for the average number of He atoms in the bubbles in the fcc lattice of the Pu-Ga alloys is 180 He atoms and the radius $R = 0.7\ nm$.

4) Calculated in CMD simulations He bubble radius distribution function is compared to one observed experimentally [14]. Although the overall behavior of the experimental and calculated distributions is quite similar there are some differences. The plausible explanations for that differences are discussed in Section 4. The possible influence of Ga concentration on the equilibrium parameters of the bubbles requires additional CMD calculations.

At the first glance it looks like that there is the contradiction between the estimates of the equilibrium bubble radius obtained by two sets of calculations in Section 3 - $R = 1.1\ nm$ and in Section 4 - $R = 0.8\ nm$. The difference is caused by the fact that in the calculations we investigated two different mechanisms of He bubble growth. The first one is the bubble coarsening by the diffusive motion of secluded He atom-vacancy complexes, and the second - the growth by coalescence of smaller bubbles. Our CMD calculations and experimental TEM observations [14] demonstrated that the existence of He atoms in the form of single He atom-vacancy complexes is thermodynamically unfavoured. Although the single He atom-vacancy complex is the initial state of the He atom just after the α-decay the experimental TEM observations and our CMD simulations evidence that if two diffusing He atom-vacancy complexes meet or He atom-vacancy complex meets another bubble they would join, and a nucleus of He gas bubble would be formed. Moreover, it is thermodynamically profitable to form the bubbles with He atom concentration $2 - 3$ He atoms per vacant site. The second mechanism of migration and coalescence of smaller bubbles have been

observed by *in situ* TEM at elevated temperatures as the dominant mechanism of He bubbles growth [16]. Of course at the finite temperatures both of these mechanisms can exist, but statistical weight of the first one and its contribution to the overall radius distribution function is much smaller than that of the MC mechanism. Thus, the second estimate $R = 0.8\,nm$ of the equilibrium He bubble radius is more reasonable and related to the overall thermodynamic behavior of helium in the fcc lattice of δ-phase Pu-Ga alloys.

Note once more that all the described CMD calculations were done for ambient conditions which approximately correspond to material storage conditions. It is interesting to repeat the presented calculations for elevated and reduced temperatures to quantify the effect of temperature on the equilibrium parameters of He bubbles as it was done experimentally in [16].

The presented results of the CMD simulations for the calculation of thermodynamic potentials and determination of relative thermodynamic stability of various micro-configurations of systems with artificially introduced systems of defects allow to conclude that the TIM technique is applicable for the study of thermodynamics and predictions of behavior of defects whose dynamics is inaccessible by direct CMD modeling. The presented approach can be applied to other materials and kinds of defects, for example, we used the described method of investigations to study relative thermodynamic stability of vacancy complexes and their interaction with preexisting extended defects in the δ-phase Pu-Ga alloys (to be published elsewhere).

We have also to notice two significant shortcomings of the presented approach to the determination of relative thermodynamic preference of various micro-configurations. While the approach provides the answer which of the examined micro-states is preferable from the standpoint of thermodynamics it does not predict the most thermodynamically stable state if this was not included in the calculation set. In this sense the result of calculations depends on "imagination" and "physics flair" of a researcher, meaning that one should generate the micro-configurations for the simulations based on preliminary understanding and available experimental information about the problem. The second

disadvantage of the presented pathway is coming from the equilibrium thermodynamics approach. The approach answers which of micro-configurations is more thermodynamically stable, but does not answer the questions how fast and how (if at all) will the system transfer from one micro-configuration to another? The kinetics of transitions (in our case the kinetics of Helium bubble growth) can not be resolved by the equilibrium thermodynamics methods.

6. Acknowledgments

The work was performed through the collaboration authorized under Contract No. B593480 between Russian Federal Nuclear Center - Zababakhin Institute of Technical Physics (RFNC-VNIITF) and Lawrence Livermore National Laboratory.

Prepared by LLNL under Contract DE-AC52-07NA27344

References

[1] W. G. Wolfer, Los Alamos Sci. 26(2) (2000) 274–285.

[2] S. S. Hecker, J. C. Martz, Plutonium aging: from mystery to enigma, in: L. G. Mallinson (Ed.), Aging Studies and Lifetime Extension of Materials, Kluwer Academic, New York, 2001, pp. 23–52.

[3] D. L. Clark, S. S. Hecker, G. D. Jarvinen, M. P. Neu, in: L. R. Morss, N. Edelstein, J. Fuger, J. J. Katz (Eds.), The Chemistry of the Actinide and Transactinide Elements, 3rd Edition, Springer, 2006, Ch. 7, pp. 979–989.

[4] W. G. Wolfer, A. Kubota, P. Soderlind, A. I. Landa, B. Oudot, B. Sadigh, J. B. Sturgeon, M. P. Surh, Density changes in ga-stabilized delta-pu, and what they mean, Journal of Alloys and Compounds 444-445 (2007) 72 – 79.

[5] R. H. Howell, P. A. Sterne, J. Hartley, T. E. Cawan, Appl. Surf. Sci. 149 (1999) 103–105.

[6] B. D. Wirth, A. J. Shwartz, M. J. Fluss, M. J. Cartula, M. A. Wall, W. G. Wolfer, Mat. Sci. Soc. Bull. 26(9) (2001) 679–684.

[7] S. M. Valone, M. I. Baskes, R. L. Martin, Phys. Rev. B 73 (2006) 214209.

[8] V. V. Dremov, F. A. Sapozhnikov, A. L. Kutepov, V. Anisimov, M. Korotin, A. Shorikov, D. L. Preston, M. A. Zocher, Atomistic simulations of helium dynamics in a plutonium lattice, Phys. Rev. B 77 (2008) 224306.

[9] D. L. Rohr, K. P. Staudhammer, J. Nucl. Mater. 144 (1987) 202–204.

[10] T. G. Zocco, D. L. Rohr, Development in tem examination of pu and pu alloys, Vol. 115 of Mater. Res. Soc. Symp. Proc., MRS, Pittsburgh, PA, 1988.

[11] K. T. Moore, M. A. Wall, , A. J. Schwartz, J. Nucl. Mater. 306 (2002) 213.

[12] J. C. Martz, A. J. Schwartz, J. Metals 55(9) (2003) 19–23.

[13] T. G. Zocco, A. J. Schwartz, J. Metals 55(9) (2003) 24–27.

[14] A. J. Schwartz, M. A. Wall, T. G. Zocco, W. G. Wolfer, Characterization and modeling of helium bubbles in self-irradiated plutonium alloys, Philos. Mag. 85 (2005) 479–488.

[15] K. T. Moore, Micron 41 (2010) 336.

[16] J. R. Jeffries, M. A. Wall, K. T. Moore, A. J. Schwartz, He bubble coarsening by migration and coalescence in annealed pu-ga alloys, J. Nucl. Mater. 410 (2011) 84–88.

[17] H. Schroeder, P. F. P. Fichtner, J. Nucl. Mater. 179-181 (1991) 1007.

[18] A. Baldan, J. Mater. Sci. 37 (2002) 2171.

[19] E. E. Gruber, J. Appl. Phys. 38 (1967) 243.

[20] M. I. Baskes, A. C. Lawson, S. M. Valone, Lattice vibrations in delta-plutonium: Molecular dynamics calculations, Phys. Rev. B 72 (2005) 014129.

[21] V. V. Dremov, A. V. Karavaev, S. I. Samarin, F. A. Sapozhnikov, M. A. Zocher, D. L. Preston, Molecular dynamics characterization of thermodynamic and mechanical properties of Pu as dependent upon alloying additions and defects concentration. Part I, J. Nucl. Mater. 385 (2009) 79–82.

[22] D. Frenkel, A. J. C. Laad, J. Chem. Phys. 81 (1984) 3188.

[23] D. Frenkel, Free energy computation and first-order pase transitions, in: Molecular Dynamics Simulations of Statistical Mechanics Systems, XCVII, Soc. Italiana di Fisica, Bologna, Italy, 1986.

[24] D. Frenkel, B. Smit, Understanding Molecular Simulations. From Algorithms to Applications, Academic Press, San Diego, 2002.

[25] L. D. Landau, E. M. Lifshits, Theoretical Physics. Statistical Physics, 2nd Edition, Vol. V, Nauka, Moscow, 1964, in Russian.

[26] R. Kubo, Statistical Mechanics. An Advanced Course with Problems and Solutions, North-Holland Publishing Company, Amsterdam, 1965.

[27] M. I. Baskes, Modified embedded-atom potentials for cubic materials and impurities, Phys. Rev. B 46 (1992) 2727.

[28] M. I. Baskes, R. A. Johnson, Modeling Simul. Mater. Sci. Eng. 2 (1994) 147–163.

[29] M. I. Baskes, J. E. Angelo, C. L. Bisson, Atomistic calculations of composite interfaces, Modeling Simul. Mater. Sci. Eng. 2 (1994) 505.

[30] M. I. Baskes, Atomistic model of plutonium, Phys. Rev. B 62 (2000) 15532.

[31] M. I. Baskes, S. P. Chen, F. J. Cherne, Atomistic model of gallium, Phys. Rev. B 66 (2002) 104107.

[32] M. I. Baskes, K. Muralidharan, M. Stan, S. M. Valone, F. J. Cherne, Using the modified embedded-atom method to calculate the properties of pu-ga alloys, J. of Metals. 9 (2003) 41–50.

[33] V. V. Dremov, A. V. Karavaev, F. A. Sapozhnikov, M. A. Vorobyova, D. L. Preston, M. Zocher, Molecular dynamics evaluation of the impact of Ga, He and vacancy concentration on the mechanical properties of Ga-stabilized delta-Pu, J. Nucl. Mater. 414 (2011) 471–478.

[34] H. J. C. Berendsen, J. P. M. Postma, W. F. van Gunsteren, A. DiNola, J. R. Haak, J. Chem. Phys. 81 (1984) 3684–3690.

[35] S. Nose, J. Chem. Phys. 81 (1984) 511–519.

[36] W. G. Hoover, Phys. Rev. A 31 (1985) 1695–1697.

[37] A. Arsenlis, W. G. Wolfer, A. J. Schwartz, Change in flaw stress and ductility of delta-phase pu-ga alloys due to self-irradiation damage, J. Nucl. Mater. 336 (2005) 31–39.

[38] R. Kubo, Thermodynamics. An Advanced Course with Problems and Solutions, North-Holland Publishing Company, Amsterdam, 1968.

[39] I. P. Bazarov, E. V. Gevorkyan, P. N. Nikolaev, Thermodynamics and Statistical Physics. Theory of Equilibrium Systems, Moscow State University Publishing, Moscow, 1986, in Russian.

[40] J. L. Robbins, Mechanical properties of delta-stabilized pu-1.0 wt. percent ga alloys, J. Nucl. Mater. 324 (2004) 125–133.